



# LaCoO<sub>3</sub> perovskite catalysts for the environmental application of Auto motive CO oxidation

Patel Femina and Patel Sanjay

Department of Chemical Engineering, Institute of Technology, Nirma University, Ahmedabad-382481, INDIA

Available online at: [www.isca.in](http://www.isca.in)

(Received 15<sup>th</sup> October 2011, revised 10<sup>th</sup> January 2012, accepted 25<sup>th</sup> January 2012)

## Abstract

Perovskite-type oxides were synthesized through conventional citrate methods. The synthesized perovskite materials had the nominal compositions of LaCoO<sub>3</sub>, LaCo<sub>0.8</sub>Cu<sub>0.2</sub>O<sub>3</sub>, La<sub>0.8</sub>Sr<sub>0.2</sub>CoO<sub>3</sub> and La<sub>0.8</sub>Sr<sub>0.2</sub>Co<sub>0.8</sub>Cu<sub>0.2</sub>O<sub>3</sub>. The catalytic activity of the perovskite samples (for CO oxidation) were measured using a stainless steel reactor with an inlet gas mixture containing exhaust composition as gasoline engine. The prepared perovskite samples were characterized by nitrogen adsorption (BET), EDX and XRD analyses. The perovskite catalysts showed good structural and chemical stability and high activity for the catalytic CO oxidation reaction. The catalyst samples prepared by the citrate method achieved the same CO conversion at lower temperatures than those prepared by the sol gel method. This was attributed to a better-formed perovskite crystals by the citrate method. Substituted perovskite composition showed higher activity for CO conversions higher than 90%. Hence, for the environmental application of the automotive emission control, it can completely eliminate the poisonous CO gas.

**Keywords:** Catalytic converter, perovskite, automotive emission, catalyst, citric acid method.

## Introduction

The purification of automobile exhaust gases (carbon monoxide (CO), unburned hydrocarbon (HC) and nitrogen oxides (NO<sub>x</sub>)) which can cause the green house gas effect, depletion of the ozone layer, acid rain and photochemical smog is regarded as one of the main objectives for catalytic control of air pollution<sup>1-3</sup>. Several series of catalytic materials including supported noble metals, metal oxides, mesostructured alumino-silicates, pillared clays and active carbon were investigated as catalysts for purification of automobile exhaust gases<sup>4</sup>.

These harmful components convert to inert gases such as carbon dioxide in catalytic converters before the exhaust gas emitted to the atmosphere. The catalytic converters are, in fact reactors that consist of monolithic honeycombs skeleton made of ceramic or metallic materials. This structure is then coated by a ceramic substrates impregnated with Pt, Pd and other platinum group metals (PGM) as the active catalytic sites<sup>5-7</sup>.

However, due to the rising cost of PGM, many researchers have been searching for alternative materials as the active catalytic phase. Perovskite oxides, promising alternatives to supported noble metals for exhaust gas depollution because of their low cost, thermal stability at rather high temperatures, great versatility and excellent redox properties.

The general chemical formula for perovskite compounds is ABO<sub>3</sub>, where 'A' and 'B' are two cations of very different sizes and O is an anion that bonds to both. The 'A' atoms are

larger than the 'B' atoms. A ion can be rare earth, alkaline earth, alkali and other large ions such as Pb<sup>+2</sup>, Bi<sup>+3</sup> that fits in to the dodecahedral site of the framework. The B ion can be 3d, 4d and 5d transition metal ions. The ideal cubic-symmetry structure has the B cation in 6-fold coordination surrounded by an octahedron of anions (B surrounded by six oxygen in octahedral coordination) and the A cation in 12-fold cuboctahedral coordination (A coordinated by 12 oxygen). Many metals are stable in the ABO<sub>3</sub> perovskite structure provided that the A and B cations have dimension ( $r_A > 0.90 \text{ \AA}$ ,  $r_B > 0.51 \text{ \AA}$ ) in agreement with the limits of the so-called "tolerance factor"  $t$  ( $0.8 < t < 1.0$ ) defined by Goldschmidt, as  $t = (r_A + r_O) / \sqrt{2}(r_B + r_O)$ , where  $r_A$ ,  $r_B$  and  $r_O$  are the ionic radii for A, B and O, respectively<sup>7-10</sup>.

Perovskite compounds can also tolerate significant partial substitution (A and/or B with metals A', B' correspondingly of different oxidation states i.e. AA'BO<sub>3</sub>, ABB'O<sub>3</sub> etc. or A<sub>1-x</sub>A'B<sub>1-y</sub>B'yO<sub>3±δ</sub>) and oxygen non-stoichiometry (oxygen excess as well as deficiency) indicated by the δ subscript in the formula while still maintaining the perovskite structure<sup>11-13</sup>.

The catalytic properties of perovskite-type oxides basically depend on the nature of A and B ions and on their valence state. The A site ions are catalytically inactive. The nature of these ions however also influences the stability of the perovskite phase. Catalytic activity is generally determined by the B cation. The substitution at A site with ions having lower valence can allow the formation of structural defects such as anionic or cationic vacancies and/or a change in the

oxidation state of the transition metal cation to maintain the electro neutrality of the compound. When the oxidation state of B cation increases, the relative ease of the redox process generates larger quantities of available oxygen at low temperature and the overall oxidation activity enhances. Moreover, the oxygen vacancies favour the catalytic activity in oxidation reaction because they increase the lattice oxygen mobility. Substitution with a cation with the same valence state should not lead in principle, to the occurrence of the above mentioned modifications due to the unchanged charge balance. Moreover, B-site substitution of perovskites was also considered an effective way to improve their catalytic properties due to the generation of new lattice defects, mixed valence states and nonstoichiometric oxygen.

Several synthesis methods for preparation of perovskite phases have been proposed and developed over the years. These methods include pyrolysis, co-precipitation, citrate complexation, spray-drying, freeze-drying, micro emulsion, sol-gel process etc. Among those, the benchmark methods are co-precipitation and citrate methods<sup>14-17</sup>.

Perovskite-type oxides have been widely studied in the last years as catalysts for CO oxidation due to their high activity and thermal stability. It is well documented that the oxidation activity is mainly controlled by the nature of the B-site element with Co, Mn and Fe being usually reported as the most effective metals when lanthanum is in the A-site<sup>11-13</sup>.

Synergistic effects can be a powerful tool of catalyst design and effect is due to combination of two different ions at the B-site This synergistic effect is due to bifunctional catalysis of Mn and Cu located at B site in 1:1 atomic ratio and exhibits a very high catalytic activity for CO oxidation<sup>18, 19</sup>. It has also been reported that partial substitution of transition metal at B site with other trivalent cation can be effective to enhance oxidation activity of perovskites. In particular, Zhong et al. studied  $\text{LaFe}_{1-x}\text{M}_x\text{O}_3$  (M = Al, Mn, Co) perovskites and claimed a synergistic effect due to the presence of two types of B cations which causes an increase in their average oxidation state resulting in better performances for methane oxidation<sup>20</sup>.

In this work, two synthesis methods, namely citrate method and sol gel were implemented for preparation of perovskite catalyst samples. To study the effect of Sr and Cu substitution for A and B cations in the  $\text{ABO}_3$  perovskite structure were synthesized and tested for carbon monoxide oxidation in an oxygen gas stream.

## Material and Methods

**Catalyst preparation: Citrate method (CT):** The citrate compound was prepared by complexation of the nitrate salts with citric acid. A concentrated solution of the metal nitrates was mixed with an aqueous solution of citric acid by fixing at unity the molar ratio of citric acid to the metal cations. Metal nitrates  $\text{La}(\text{NO}_3)_3 \cdot 6\text{H}_2\text{O}$ ,  $\text{Sr}(\text{NO}_3)_2$ ,  $\text{Co}(\text{NO}_3)_2 \cdot 6\text{H}_2\text{O}$ ,

$\text{Sr}(\text{NO}_3)_2$  and  $\text{Cu}(\text{NO}_3)_2 \cdot 3\text{H}_2\text{O}$ ) were first dissolved in distilled water (25 ml). Citric acid (10% excess over the number of ionic equivalents of cations) was separately dissolved in distilled water (25 ml) and added to the precursor solution under vigorous stirring for 15 min. Excess water was evaporated under slow stirring in oil bath at 80 °C until a gel was obtained. The viscous gel was then dried at 100 °C overnight in hot air oven. The obtained spongy material was finely ground and calcined under air atmosphere at 750 °C for 5 h.

### Sol-Gel method using citric acid as complexing agents

**(Sol gel):** A  $\text{LaCoO}_3$  compound was synthesized by a sol-gel method employing citric acid as complexing agent. The required amounts of the precursor salts ( $\text{La}(\text{NO}_3)_3 \cdot 6\text{H}_2\text{O}$ ,  $\text{Co}(\text{NO}_3)_2 \cdot 6\text{H}_2\text{O}$ ) along with citric acid were dissolved in water at an equivalent ratio of 1:1 (metal cations : citric acid). Ethylene glycol (25 ml) and citric acid were used to make the gel. The Ethylene Glycol and citric acid were added drop-wise to the nitrate solution and they were stirred for 15 min. The resulting solutions were heated to 80 °C to form a viscous gel finally yield a solid precursor upon slow solvent evaporation at that temperature for several hours. This gel was dried in an oven at 100 °C overnight and after thorough grinding of the resulting powder, it was finally calcined under air at 750 °C for 5 h in order to achieve the corresponding perovskite structure in the samples.

**X-ray Diffraction:** Phase analysis, lattice parameters and particle sizes were determined by X-ray diffraction (XRD) using PW1774 Spinner Diffractometer system XPERT-MPD operated at 40 kV and 30 mA with Ni-filtered Cu K $\alpha$  radiation ( $\lambda = 1.5406 \text{ \AA}$ ). Spectra were recorded with step scans from 2° to 99° in 2 $\theta$  angle and 1 s for each 0.05° step. Lattice parameters were calculated from the reflections appearing in the 2 $\theta = 2-99^\circ$  range using the software program. The identification of the crystal phases took place using the JCPDS (Joint committee on Powder diffraction standards) data bank.

Particle sizes ( $D$ ) were calculated by means of the Scherrer equation  $D = K\lambda/\beta\cos \theta$  after Warren's correction for instrumental broadening.  $K$  is a constant equal to 0.9,  $\lambda$  the wavelength of the X-ray used,  $\beta$  the effective linewidth of the observed X-ray reflection, calculated by the expression  $\beta^2 = B^2 - b^2$  (where  $B$  is the full width at half maximum (FWHM),  $b$  the instrumental broadening determined through the FWHM of the X-ray reflection at  $2\theta \approx 28^\circ$  of crystalline  $\text{SiO}_2$  with particles larger than 1000 Å,  $\theta$  the diffraction angle).

### Energy dispersive X-ray spectroscopy (EDX or EDS):

Energy Dispersive of X-Ray (EDX) of samples was carried out in JEOL made instrument JEM2100 model which has attached detector OXFORD Instrument INCA X-SIGHT model. EDX was used to investigate the morphology as well as the elemental composition and distribution of all the catalyst compositional analysis.

**BET surface area:** BET Surface area of the materials were measured by nitrogen adsorption at the liquid nitrogen temperature ( $-196^{\circ}\text{C}$ ) using a volumetric all glass apparatus. The specific surface area of the materials calcined at  $750^{\circ}\text{C}$  for 5 h was determined from nitrogen adsorption isotherms measured at  $-196^{\circ}\text{C}$  using a Micromeritics ASAP 2020 instrument. Samples were degassed at  $300^{\circ}\text{C}$  under vacuum ( $10^{-3}$  Pa) until complete removal of humidity (about 3-4 h) prior to adsorption-desorption experiments. Nitrogen adsorption measurements were performed up to a relative pressure  $P/P_0 = 1$ . The specific surface area was determined from the linear part of the BET curve. The pore size distribution was calculated from the desorption branch of  $\text{N}_2$  adsorption/desorption isotherms using the Barrett-Joyner-Halenda (BJH) formula. Pore volume and average diameter were also obtained from the pore size distribution curves using the software.

**Catalytic activity:** Before the activity tests, the catalyst in the bed was activated by passing  $\text{N}_2$  (90 %) and  $\text{O}_2$  (10 %) at  $440\text{ cm}^3\text{ min}^{-1}$  for 2 h at  $500^{\circ}\text{C}$  below the calcinations temperature to remove adsorbed moisture.

Catalytic activity in the combustion of carbon monoxide was determined using a catalyst charge of about ca. 1 g previously added with 3 g of  $\text{SiO}_2$  (0.5–1.5 mm granulate) in order to reduce the specific pressure drop across the reactor and to prevent thermal runaways placed between two ceramic blanket wool and inserted into stainless steel fixed bed reactor (I.D. 1.805 cm, O.D. 1.905 cm and L.50 cm). The reactor operated in a down flow mode at atmospheric pressure was placed in a tubular PID-regulated furnace. The reaction temperature was controlled with a K type thermocouple placed in the catalytic bed. A gas mixture 7.9 %  $\text{CO}$ , 9.64 %  $\text{O}_2$ ,  $\text{N}_2$  as balance with a total gas hourly space velocity (GHSV) of  $29000\text{ Ncm}^3\text{ g}^{-1}\text{ h}^{-1}$ . The outlet and inlet gas compositions were followed using gas chromatograph equipped with Shin Carbon ST Micropacked column and a  $\mu\text{TCD}$  detector. Helium was used as a carrier gas at a flow of  $20\text{ ml min}^{-1}$  and the analysis is conducted isothermally at  $60^{\circ}\text{C}$ .

The CO conversion in activity tests was defined as:

$$X_{\text{CO}} = (F_{\text{f,CO}} - F_{\text{p,CO}}) / F_{\text{f,CO}}$$

$F_{\text{f,CO}}$ : Molar flow rate of CO in feed stream,  $F_{\text{p,CO}}$ : Molar flow rate of CO in product stream

## Results and Discussion

**Catalyst characterization:** XRD measurement of  $\text{LaCoO}_3$ ,  $\text{LaCo}_{0.8}\text{Cu}_{0.2}\text{O}_3$ ,  $\text{La}_{0.8}\text{Sr}_{0.2}\text{CoO}_3$  and  $\text{La}_{0.8}\text{Sr}_{0.2}\text{Co}_{0.8}\text{Cu}_{0.2}\text{O}_3$  (calcined at  $750^{\circ}\text{C}$  for 5 h) were prepared by citrate method,  $\text{LaCoO}_3$  prepared by sol gel method (calcined at  $750^{\circ}\text{C}$  for 5 h) and its XRD patterns are presented in figure - 1. The comparison of these spectra with JCPDS charts indicates that all Co based samples except  $\text{La}_{0.8}\text{Sr}_{0.2}\text{CoO}_3$  are essentially

perovskites type mixed oxides (JCPDC card 00-025-1060, 00-006-0491). Other phases such as  $\text{SrCoO}_{2.8}$  (JCPDS card 00-039-1084) in the case of  $\text{La}_{0.8}\text{Sr}_{0.2}\text{CoO}_3$  was detected in addition to the major  $\text{ABO}_3$  Perovskite phase.

Phase formation is closely related to the calcination temperature. At  $750^{\circ}\text{C}$ , all the catalyst samples except  $\text{La}_{0.8}\text{Sr}_{0.2}\text{CoO}_3$  completely transformed lanthanum and cobalt nitrates into  $\text{LaCoO}_3$  perovskite phase. No spinel phase  $\text{La}_2\text{CoO}_4$  (that normally tends to form at higher temperatures) was observed in these samples.

Moreover, a small shift of diffraction peaks in XRD patterns of Cu substituted samples to low diffraction angle ( $2\theta$ ) with respect to unsubstituted one implied that Cu had indeed been introduced into the perovskite lattice. The crystallite sizes of prepared perovskites calculated by Scherrer's equation after Warren's correction of instrumental broadening are also reported in table - 1.

The results for the nitrogen isothermal sorption at 77 K for  $\text{LaCoO}_3$ ,  $\text{LaCo}_{0.8}\text{Cu}_{0.2}\text{O}_3$  perovskite- type mixed oxides prepared by citrate method and  $\text{LaCoO}_3$  prepared by sol gel method are presented in figure - 2, respectively. All the isothermal results show hysteresis loops, whose characteristics exhibit dependence on the structure of the samples which are confirmed to be with a porous morphology. The specific surface area (BET surface area), pore size and pore volume of the samples synthesized by citrate method and sol gel method after calcinations at  $750^{\circ}\text{C}$  for 5 h are listed in table - 1.

Adsorption-desorption isotherms of the catalysts have shown similar characteristics. Barrett-Joyner-Halendar (BJH) analysis showed that catalyst pores were meso size and the average pore sizes were found to be in between 2 and 27 nm.

**Catalytic oxidation of CO:** The catalytic activity of the perovskite samples chiefly depends on three factors: chemical composition, degree of crystallinity and the crystals morphology (including particle sizes, pore size distribution and specific surface area of the perovskite catalyst). All these factors are affected by the synthesis method and the specific synthesis operating conditions.

The temperature corresponding to 50% conversion of CO is defined as the catalyst "light off" temperature and it is an important parameter in catalytic reactions. The lower the light off temperature, the more active the catalyst is. The light off temperature for a catalyst prepared by citrate method is around  $420^{\circ}\text{C}$  for CO conversion (shown in figure - 3) in case of  $\text{LaCoO}_3$  prepared by citrate method which lower than the perovskite prepared by sol gel. The enhancement of catalytic activity may attribute to both the higher BET surface of the perovskite used and large number of active sites available in case of citrate method.

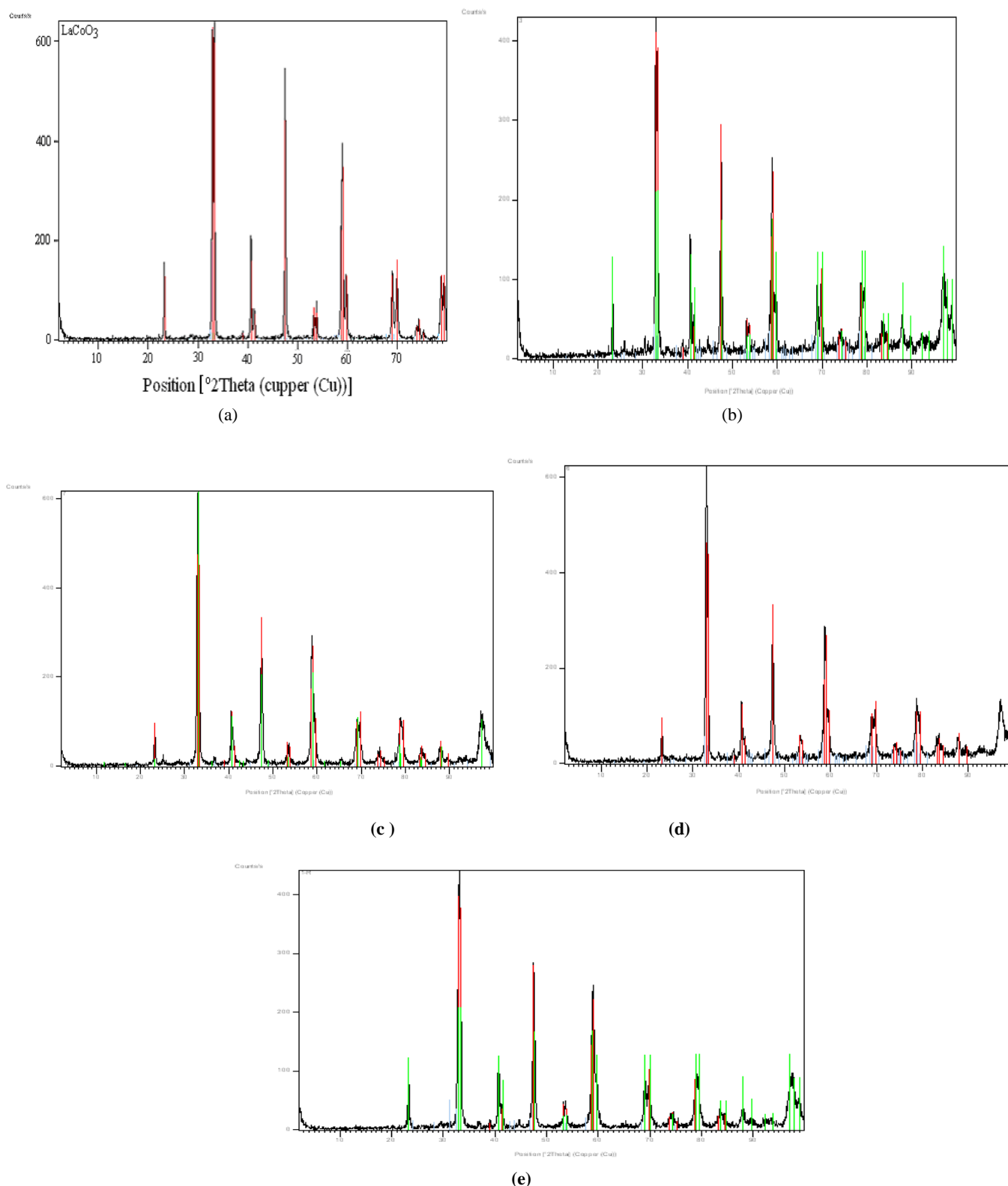


**Figure - 1**  
XRD patterns of (a)  $\text{LaCoO}_3$  by CT (b)  $\text{LaCo}_{0.8}\text{Cu}_{0.2}\text{O}_3$  by CT (c)  $\text{La}_{0.8}\text{Sr}_{0.2}\text{CoO}_3$  by CT (d)  $\text{La}_{0.8}\text{Sr}_{0.2}\text{Co}_{0.8}\text{Cu}_{0.2}\text{O}_3$  by CT and (e)  $\text{LaCoO}_3$  by sol gel

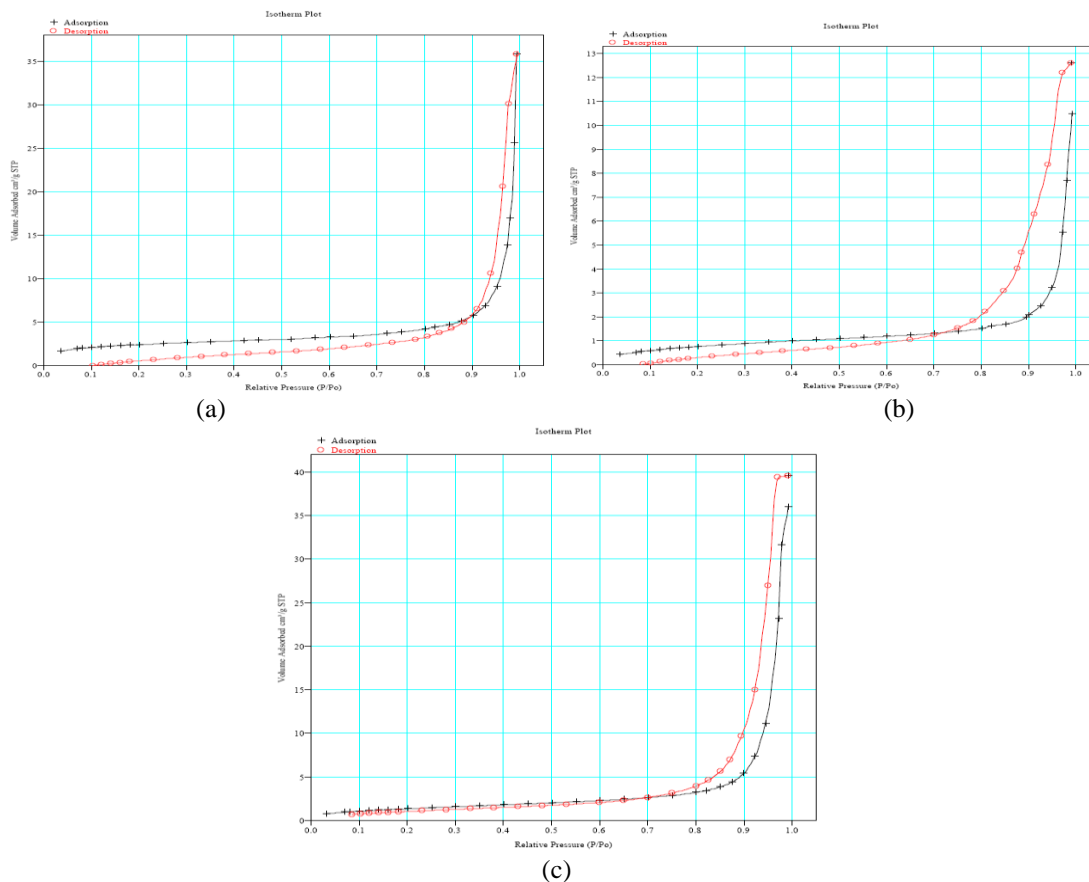


**Figure - 2**  
N<sub>2</sub> adsorption-desorption isotherm of (a) LaCoO<sub>3</sub> by CT  
(b) LaCo<sub>0.8</sub>Cu<sub>0.2</sub>O<sub>3</sub> by CT (c) LaCoO<sub>3</sub> by sol gel

**Table - 1**  
Properties of Co-based catalysts after calcinations at 750 °C for 5 h

Sr. No.	Sample	Calcination T	Crystallite Size (nm)	Phases	Specific Surface area (m <sup>2</sup> /g)	Pore diameter (nm)	Pore volume (cm <sup>3</sup> /g)
1	LaCoO <sub>3</sub>	750 °C	35-56	P	8.78	9.77	0.0214
2	LaCo <sub>0.8</sub> Cu <sub>0.2</sub> O <sub>3</sub>		29-42	P	3.04	11.29	0.0086
3	La <sub>0.8</sub> Sr <sub>0.2</sub> CoO <sub>3</sub>		25-56	P+O (SrCoO <sub>2.8</sub> )	3.91	8.32	0.0081
4	La <sub>0.8</sub> Sr <sub>0.2</sub> Co <sub>0.8</sub> Cu <sub>0.2</sub> O <sub>3</sub>		25-34	P	3.75	9.97	0.0093
5	LaCoO <sub>3</sub> (sol gel)		35-42	P	5.22	27.42	0.0358

Adding impurities to the benchmark LaCoO<sub>3</sub> perovskite sample, in general may enhance the rate of combustion due to an increase in the oxygen mobility in the bulk of the solid. Partial substitution of transition metal at B site with other cation (Cu) can be effective to enhance oxidation activity of perovskites due to synergistic effect (due to combination of two different ions at the B-site). Synergistic effect is due to the presence of two types of B cations which causes an increase in their average oxidation state resulting in better performances for carbon monoxide oxidation. This is

probably the reason that perovskite composition of LaCo<sub>0.8</sub>Cu<sub>0.2</sub>O<sub>3</sub> has resulted in the best CO oxidation performance compare to unsubstituted LaCoO<sub>3</sub> prepared by citrate method. Activity tests of the catalysts shows that LaCoO<sub>3</sub> has 50 % conversion for CO at 420 °C and the maximum conversion was found around 58% even it has large surface area due to less active site available for catalytic activity and also low residence time of the reactants in the bed.

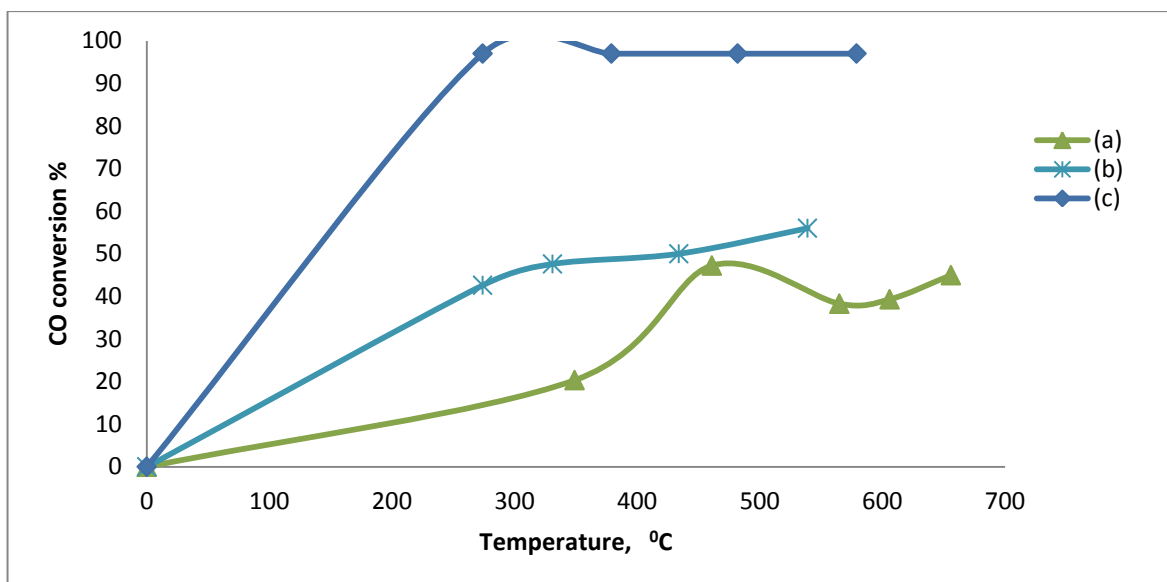


**Figure - 3**  
CO conversion as function of temperature for LaCoO<sub>3</sub> perovskites prepared by  
(a) CT : CO: 7.9 %, O<sub>2</sub> : 9.64 %, N<sub>2</sub> : 82.39 %, SV : 29000 Ncm<sup>3</sup>g<sup>-1</sup>h<sup>-1</sup>) and  
(b) Sol gel (CO: 7.9 %, O<sub>2</sub> : 9.64 %, N<sub>2</sub> : 82.39 %, SV : 29000 Ncm<sup>3</sup>g<sup>-1</sup>h<sup>-1</sup>),  
(c) LaCo<sub>0.8</sub>Cu<sub>0.2</sub>O<sub>3</sub> by CT : CO : 6.8 %, O<sub>2</sub> : 17.6 %, N<sub>2</sub> : 85.67 %, SV = 48810 Ncm<sup>3</sup>g<sup>-1</sup>h<sup>-1</sup>

## Conclusion

Perovskite samples were synthesized by the citrate (LaCoO<sub>3</sub>, LaCo<sub>0.8</sub>Cu<sub>0.2</sub>O<sub>3</sub>, La<sub>0.8</sub>Sr<sub>0.2</sub>CoO<sub>3</sub> and La<sub>0.8</sub>Sr<sub>0.2</sub>Co<sub>0.8</sub>Cu<sub>0.2</sub>O<sub>3</sub>) and sol gel (LaCoO<sub>3</sub>) methods and tested toward CO oxidation reaction using a gas mixture. Various characterization techniques confirmed that the citrate method produces lower crystallinity and higher surface area than the sol gel method. The oxidation catalytic activity of the substituted samples produced by the citrate method was higher than the samples produced by sol gel due to synergistic effect in case of substituted catalyst.

## Acknowledgement

The work described above was fully supported by a research grant from the Nirma University.

## References

- Shinjoh H., Rare earth metals for automotive exhaust catalysts, *Journal of Alloys and Compounds*, **408-412**, 1061-1064 (2006)
- Thakur Prabhat, Rahul Mathur Anil and Balomajumder Chandrajit, Biofiltration of volatile organic compounds (VOCs) – An overview, *Research Journal of Chemical Sciences*, **1(8)**, 83-92 (2011)
- Heck R. and Farrauto R., Automobile exhaust catalysts, *Applied Catalysis A: General*, **221**, 443-457 (2001)
- Traa Y., Burger B. and Weitkamp J., Zeolite-based materials for the selective catalytic reduction of NO<sub>x</sub> with hydrocarbons, *Microporous and Mesoporous Materials*, **30**, 3-41 (1999)
- Zhang R., Villanueva A., Alamdari H. and Kaliaguine S., Catalytic reduction of NO by propene over LaCo<sub>1-x</sub>Cu<sub>x</sub>O<sub>3</sub> perovskites synthesized by reactive grinding, *Applied Catalysis B: Environmental*, **64**, 220-233 (2006)
- Seyfi B., Baghalha M. and Kazemian H., Modified LaCoO<sub>3</sub> nano-perovskite catalysts for the environmental application of automotive CO oxidation, *Chemical Engineering Journal*, **148**, 306-311 (2009)
- Sharma S., Hegde M., Das R. and Pandey M., Hydrocarbon oxidation and three-way catalytic activity on a single step directly coated cordierite monolith: High catalytic activity of Ce<sub>0.98</sub>Pd<sub>0.02</sub>O<sub>2</sub>, *Applied Catalysis A: General*, **337**, 130-137 (2008)
- H. Iwakuni, Shinmyou Y., Yano H., Matsumoto H. and Ishihara T., Direct decomposition of NO into N<sub>2</sub> and O<sub>2</sub> on BaMnO<sub>3</sub> – based perovskites oxides, *Applied Catalysis B: Environmental*, **74**, 299-306 (2007)

9. Ciambelli P., Cimino S., De Rossi S., Lisi L., Minelli G., Porta P. and Russo G.,  $AFeO_3$  (A= La, Nd, Sm) and  $LaFe_{1-x}Mg_xO_3$  perovskites as methane combustion and CO oxidation catalysts: structural, redox and catalytic properties, *Applied Catalysis B: Environmental*, **29**, 239–250 (2001)
10. Ciambelli P., Cimino S., Lisi L., Faticanti M., Minelli G., Pettiti I. and Porta P., La, Ca and Fe oxide perovskites: preparation, characterization and catalytic properties for methane combustion, *Applied Catalysis B: Environmental*, **33**, 193–203 (2001)
11. Alifanti M., Blangenois N., Florea M. and Delmon B., Supported Co-based perovskites as catalysts for total oxidation of methane, *Applied Catalysis A: General*, **280**, 255–265 (2005)
12. Thomas Screen, Platinum group metal perovskite catalysts – Preparation and Application, *Platinum Metals Review*, **51(2)**, 87–92 (2007)
13. Nishihata Y., Cleaning up catalyst, News and views, *Nature*, **418**, 138 (2002)
14. Zhang R., Alamdari H. and Kaliaguine S., Fe-based perovskites substituted by copper and palladium for NO+ CO reaction, *Journal of Catalysis*, **242**, 241–253 (2006)
15. Asuman C., Canan K., Askar K. and Nesrin O., Catalytic Combustion of Methane over  $La_aCe_\beta Co_{(2-\alpha-\beta)}O_{3\pm\delta}$  Perovskite Catalysts, *Third European combustion meeting ECM*, (2007)
16. Paolo C., Stefano C., Sergio D., Marco F., Luciana L., Giuliano M., Ida P., Piero P., Gennaro R. and Maria T.,  $AMnO_3$  (A=La, Nd, Sm) and  $Sm_{1-x}SrMnO_3$  perovskites as combustion catalysts: structural, redox and catalytic properties, *Applied Catalysis B: Environmental*, **24**, 243–253 (2000)
17. Ozuomba J. O. and Ekpunobi A. J., Sol-Gel Derived Carbon Electrode for Dye-Sensitized Solar Cells, *Research Journal of Chemical Sciences*, **1(8)**, 76-79 (2011)
18. Tanakaa H. and Misono M., Advances in designing perovskite catalysts, *Current Opinion in Solid State and Materials Science*, **5**, 381–387 (2001)
19. Strobel R., Baiker A. and Pratsinis S. E., Aerosol flame synthesis of catalysts, *Advanced Powder Technology*, **17(5)**, 457–480 (2006)
20. Lima R. K. C. de , Batista M. S., Wallau M., Sanches E. A. , Mascarenhas Y. P. and Urquieta-Gonza lez E. A. lez, High specific surface area LaFeCo perovskites — Synthesis by nanocasting and catalytic behavior in the reduction of NO with CO, *Applied Catalysis B: Environmental* , **90**, 441–450 (2009)